Vol. 150: 1–16, 2022
https://doi.org/10.3354/dao03668

DISEASES OF AQUATIC ORGANISMS
Dis Aquat Org

Published online July 7[§]

Amoebic crab disease (ACD) in edible crab *Cancer pagurus* from the English Channel, UK

K. S. Bateman[1,2,*], G. D. Stentiford[1,2], R. Kerr[1,2], C. Hooper[1,2], P. White[1], M. Edwards[1], S. Ross[1], R. Hazelgrove[1], C. Daumich[1], M. J. Green[1], D. Ivory[1], C. Evans[1], D. Bass[1,2,3]

[1]International Centre of Excellence for Aquatic Animal Health, Centre for Environment, Fisheries and Aquaculture Science (Cefas), Barrack Road, The Nothe, Weymouth DT4 8UB, UK

[2]Sustainable Aquaculture Futures, Biosciences, College of Life and Environmental Sciences, University of Exeter, Stocker Road, Exeter EX4 4QD, UK

[3]Department of Life Sciences, The Natural History Museum, Cromwell Road, London SW7 5BD, UK

ABSTRACT: The genera *Paramoeba* and *Neoparamoeba* (Amoebozoa, Dactylopodida, Paramoebidae) include well-known opportunistic pathogens associated with fish (*N. peruans*; amoebic gill disease), lobsters, molluscs and sea urchins, but only rarely with crabs (grey crab disease of blue crabs). Following reports of elevated post-capture mortality in edible crabs *Cancer pagurus* captured from a site within the English Channel fishery in the UK, a novel disease (amoebic crab disease, ACD) was detected in significant proportions of the catch. We present histopathological, transmission electron microscopy and molecular phylogenetic data, showing that this disease is defined by colonization of haemolymph, connective tissues and fixed phagocytes by amoeboid cells, leading to tissue destruction and presumably death in severely diseased hosts. The pathology was strongly associated with a novel amoeba with a phylogenetic position on 18S rRNA gene trees robustly sister to *Janickina pigmentifera* (which groups within the current circumscription of *Paramoeba*/*Neoparamoeba*), herein described as *Janickina feisti* n. sp. We provide evidence that *J. feisti* is associated with ACD in 50% of *C. pagurus* sampled from the mortality event. A diversity of other paramoebid sequence types, clustering with known radiations of *N. pemaquidensis* and *N. aestuarina* and a novel *N. aestuarina* sequence type, was detected by PCR in most of the crabs investigated, but their detection was much less strongly associated with clinical signs of disease. The discovery of ACD in edible crabs from the UK is discussed relative to published historical health surveys for this species.

KEY WORDS: *Paramoeba* · *Neoparamoeba* · Paramoebiasis · *Cancer pagurus* · *Janickina feisti* · Amoebic crab disease · ACD

1. INTRODUCTION

Paramoebiasis is caused by opportunistic amoebae belonging to the family Paramoebidae. These amoebae have been implicated with mass mortalities in farmed fish, wild crustaceans and wild sea urchins, potentially with increasing frequency (Nowak & Archibald 2018). *Paramoeba* and *Neoparamoeba* are free-living marine amoebae distinguished primarily on the basis of their cell surface coats: the former with boat-shaped microscales, and the latter with a dense amorphous glycocalyx, ca. 10 nm thick (Page 1987). However, subsequent microscopic investigations of a larger number of related lineages, combined with phylogenetic analyses have suggested that the 2 'genera' do not form holophyletic clades, that the presence or absence of microscales is not a distinguishing feature, and therefore *Neoparamoeba*

*Corresponding author: kelly.bateman@cefas.co.uk

[§]Corrections were made after publication. For details see www.int-res.com/articles/dao_oa/d150p085.pdf
This corrected version: July 28, 2022

Publisher: Inter-Research · www.int-res.com

is a junior synonym of *Paramoeba* (Feehan et al. 2013). However, due to the limited number of scale-bearing *Paramoeba* species, it has been considered premature to make these taxonomic conclusions (Kudryavtsev et al. 2011, Young et al. 2014, Volkova & Kudryavtsev 2017, Nowak & Archibald 2018, Volkova et al. 2019), and here we adhere to the nomenclature recommended by Kudryavtsev et al. (2021). Molecular data recently generated from *Janickina pigmentifera*, a parasite of marine arrow worms (Volkova & Kudryavtsev 2021), further complicate the taxonomy of paramoebids, as this genus is now shown to branch within the clade that includes *Neoparamoeba* and *Paramoeba*.

Multiple paramoebid species have been described: *N. perurans*, *N. pemaquidensis*, *N. aestuarina*, *N. branchiphila*, *N. longipodia*, and *P. eilhardi*, *P. karteshi*, *P. aparasomata*, *P. atlantica*, *P. invadens*, *P. perniciosa* and *P. schaudini* (De Faria et al. 1922, Sprague et al. 1969, Page 1970, Jones 1985, Dyková et al. 2005, Young et al. 2007, Kudryavtsev et al. 2011, 2021, Volkova & Kudryavtsev 2017, Volkova et al. 2019), all from marine or brackish habitats. Most paramoebae possess an intracellular kinetoplastid symbiont, *Perkinsela* (Dyková et al. 2003), which co-evolves with the amoeba host by vertical inheritance (Nowak & Archibald 2018). The only known exception to this is *Paramoeba aparasomata*, which has apparently lost the symbiont (Volkova et al. 2019).

Grassi (1881) identified 2 species of amoeba in marine arrow worms (Chaetognatha), noting the presence of an intracellular structure within spherical shaped cells with hyaline protrusions. These cells displayed monopodial locomotion and were named *Amoeba pigmentifera* and *A. chaetognathi*. Janicki (1912) reisolated these species, confirming the presence of an intracellular endosymbiont and moved them to *Paramoeba*. Chatton (1953) re-evaluated the structural and locomotive differences of *P. pigmentifera* and *P. chaetognathi* (Janicki 1912) and suggested they should be moved into a separate genus, establishing *Janickina* and renaming the species (*J. pigmentifera* and *J. chaetognathi*). This distinction was recently confirmed using molecular phylogenetics by Volkova & Kudryavstev (2021), who highlighted that *J. pigmentifera* has not been found as a free-living organism, suggesting it is an obligate parasite, the only example of which so far reported within the Paramoebidae. They suggested that the differences in morphology and locomotion between *Janickina* and *Neoparamoeba*/*Paramoeba* (hereafter *Neo*/*Paramoeba*) may be a consequence of this adaptation.

Three *Paramoeba* species have been reported infecting crustaceans: *P. perniciosa* in blue crab *Callinectes sapidus*, *N. pemaquidensis* in American lobster *Homarus americanus* and *Paramoeba* sp. in Pacific white shrimp *Penaeus vannamei* (Sprague et al. 1969, Mullen et al. 2005, Han 2019). Grey crab disease was first reported by Sprague & Beckett (1966) in blue crabs from Chincoteague Bay, Maryland, and Wachapreague, Virginia, USA. The disease was named due to the grey, translucent colouration of the body and appendages of moulting crabs, which were reported to be lethargic and partial to rapid mortality following removal from the water. Body fluid from these crabs contained amoeboid cells with 2 visible nucleus-like bodies. Sprague et al. (1969) isolated the amoeboid cells from crabs taken directly from the fishery and soft crabs from onshore holding facilities, naming the pathogen *Paramoeba perniciosa* (for which no sequence data are currently available). Johnson (1977) reported that this parasite affected the connective tissues and haemal spaces, only invading the circulating blood when the infection was terminal. Lighter-grade infections were not reported to affect crabs, whilst heavier infection resulted in lethargy and loss of clotting ability of the haemolymph. Johnson (1977) also reported amoebae in the haemal spaces of the antennal gland and Y organ, connective tissues of the midgut and haemal spaces of the hepatopancreas. In terminal-stage infections, amoeba cells were reported in the haemal spaces of the gills, heart, nerve, muscle tissue and fixed phagocytes. It was noted that most infected crabs displayed a host response to the presence of the amoeba cells, involving encapsulation and destruction of these cells by host haemocytes (Johnson 1977). The disease is thought to have had local or regional effects on blue crab abundance and distribution over short periods of time. Newman & Ward (1973) sampled 30 crabs each month from various regions along the Atlantic coast of the USA, highlighting peak infections of 17% in Chincoteague Bay and 30% in North Carolina, and 100% mortality of infected animals held in tanks. Reports of grey crab disease have been rare since 1977 (Morado 2011), but similar amoebae species have been reported in other crab and lobster species, including rock crab *Cancer irroratus*, American lobster, and shore crab *Carcinus maenas* (Sawyer 1976, Sawyer & MacLean 1978, Bower et al. 1994).

Mullen et al. (2004) reported a mass mortality of American lobsters from Long Island Sound, USA, from 1999. Eleven million lobsters were estimated to have died during this event, decimating the lobster

fishery and resulting in the collapse of the regional fishing economy. At the same time, increased mortalities in crab and sea urchins from the same area were reported. Moribund lobsters were described as flaccidly paralysed, showed delayed clotting of haemolymph, red discolouration of muscle and haemolymph, and swelling of segmental ganglia of the ventral nerve cord. Samples for histology revealed a protozoan parasite within foci of haemocytic infiltration of the nerve tissues and within the subcuticular interstitium and tegumental glands. The parasite was subsequently recognised as *Neoparamoeba pemaquidensis* (Mullen et al. 2005). A sequence (represented by GenBank Acc. No. MG761752) clearly belonging to *N. pemaquidensis* has also been amplified from shore crabs from the Faroe Islands (Bojko et al. 2018).

Han (2019) described the first *Paramoeba* sp. from cultured Pacific white shrimp in a hatchery in North America. Infected animals showed reduced appetite, lethargy, respiratory distress, eroded carapace and blackened gills. Histology revealed an amoeba-like pathogen mainly affecting the gills but associated with other organs such as the lymphoid organ, antennal gland, appendages and nerve cord. Irregularly shaped trophozoites with a prominent centrally located nucleus and associated *Perkinsela*-like organism suggested that this pathogen was related to the order Dactylopodida, possibly a *Paramoeba* species. The SSU rDNA sequence of this parasite (KU852700) is very short (131 bp) and covers a region of the gene that is conserved between many paramoebid species, and therefore cannot be used for phylogenetic or taxonomic assignment. Han (2019) suggested this infection was likely due to stress factors (increased water temperature, high salinity) combined with high densities of shrimp in ponds and could be a new *Paramoeba* species infecting cultured shrimp.

The edible crab *Cancer pagurus* fishery in the UK supplies over 50% of total European catch for this species. In 2019 the value of landings into the UK was £71 million (€82.2 million) (https://www.gov.uk/government/statistics/uk-sea-fisheries-annual-statistics-report-2019), with trap-based landings supplying 31 000 of the 50 000 t landed from across Europe (www.fao.org/fishery/statistics/en, accessed 26/07/21). Diseases within commercially exploited crab stocks and the impact of such infections upon the fisheries have been highlighted (Bonami & Zhang 2011, Stentiford 2012, Lafferty et al. 2015). Stentiford (2008) reviewed diseases within *C. pagurus* populations; a number of these were reported in UK stocks including those of viral (Corbel et al. 2003, Bateman & Stentiford 2008), bacterial (Vogan et al. 2002), protistan (Stentiford et al. 2002, Stentiford et al. 2007, Feist et al. 2009, Hartikainen et al. 2014, Bateman et al. 2016), fungal (Stentiford et al. 2003) and metazoan (Boschma 1955, Kuris et al. 2002, Saville & Irwin 2005) origin. Bateman et al. (2011) highlighted that the prevalence of these diseases often differs between fished and non-fished (juvenile) populations, with juvenile crabs displaying a much broader range of pathogens than that observed in fished (adult) populations.

Following reports of elevated post-capture mortality in edible crabs captured from a site within the English Channel fishery in the UK in autumn 2019, samples were obtained for disease investigation. A high proportion of the crabs obtained were infected by amoeboid cells, accompanied by a significant host haemocytic response in some animals. We report the first recorded incidence of paramoebiasis in *C. pagurus*, principally associated with a novel paramoebid lineage belonging to the genus *Janickina*, which was strongly associated with histopathological responses in infected hosts. We name this condition amoebic crab disease (ACD) as exemplified by this disease in populations of edible crab from the English Channel fishery and describe the novel paramoebid parasite as its primary causative agent, in the context of other paramoebae associated with the diseased animals.

2. MATERIALS AND METHODS

2.1. Sampling

Thirty edible crabs were obtained from a commercial fisherman operating out of Selsey, Hampshire, in the English Channel (2.5–3 miles [~4–4.8 km] off the coast of Selsey Bill in International Council for the Exploration of the Sea [ICES] Sub Rectangle 30E9) in October 2019. An additional 22 crabs were sampled from the same location in November 2019. Crabs were selected from the landings of a single fishing vessel, sampling the first 30 animals above minimum landing size. In line with conventional practice, the arthrodial membrane of the claws had been severed ('nicked') during the period between capture and landing. In December 2020, we obtained 20 edible crabs from a location similar to that previously sampled, and an additional 26 crabs were sourced from a crab holding facility (pre-market) in the vicinity of the original landings. A total of 98 crabs were obtained.

Crabs were transported live to the Cefas Weymouth laboratory where they were humanely eutha-

nised using the Crustastun™ electrical stunning device, prior to dissection. Hepatopancreas, gill, heart, gonad and muscle tissues were removed and fixed in Davidson's seawater fixative for histology. Additional samples of hepatopancreas, heart and gill were fixed in 2.5% glutaraldehyde in 0.1 M sodium cacodylate buffer for electron microscopy. A parallel set of samples were obtained from these organs and tissues and fixed in 100% ethanol for subsequent molecular analysis.

2.2. Histology

Samples were fixed in Davidson's seawater fixative for a minimum of 24 h before transfer to 70% industrial denatured alcohol (ethyl alcohol solution, Pioneer Research Chemicals). Fixed samples were processed to wax in a vacuum infiltration processor (Leica Peloris) using standard protocols. Sections were cut at a thickness of 3–5 µm on a rotary microtome prior to mounting on glass slides before staining with haematoxylin and eosin (H&E). Stained sections were analysed by light microscopy (Nikon Eclipse Ni), and digital images and measurements were obtained using the NIS-Elements Imaging Software (Nikon).

2.3. Transmission electron microscopy (TEM)

Samples were fixed in 2.5% glutaraldehyde in 0.1 M sodium cacodylate buffer for 1 hour and rinsed in sodium cacodylate buffer before post fixation in 1% osmium tetroxide in sodium cacodylate buffer. Tissues were rinsed in sodium cacodylate buffer before being dehydrated through a graded acetone series and embedded within Agar 100 epoxy resin (Agar Scientific). Semithin sections (1–2 µm) were stained with toluidine blue to identify suitable target areas. Ultrathin sections (70–90 nm) of these target areas were mounted on uncoated copper grids and stained with aqueous uranyl acetate and Reynolds lead citrate (Reynolds 1963). Tissues were examined with a JEOL JEM 1400 transmission electron microscope, and digital images and measurements were obtained using an AMT XR80 camera and AMTv602 software.

2.4. DNA extraction

All samples were received in 70% ethanol, which was removed, and the samples were air dried prior to processing. The samples collected during October and November 2019 were homogenised in GMEM transport medium (Sigma Aldrich) using an Omni homogeniser to give 1/10 w/v tissue homogenate. A further 1:3 dilution was made with ATL buffer containing Proteinase K (Qiagen), and the sample was digested overnight at 56°C. DNA was extracted from 200 µl of the digested sample using a Qiacube HT bio-robot (Qiagen) and the Qiacube HT DNA tissue kit (Qiagen). The DNA was eluted in a 200 µl volume. Samples (40 mg) collected during December 2020 were diluted in 800 µl Lifton's buffer and 20 µl of 10 mg ml^{-1} Proteinase K (Nishiguchi et al. 2002) before homogenisation using a FastPrep-24™ Classic Instrument (MP Biomedicals™) and lysing matrix A tubes (MP Biomedicals™). DNA was extracted from 100 µl homogenate using a Maxwell® RSC Tissue DNA Kit (Promega) on a Maxwell® RSC 48 Instrument (Promega) eluting into 100 µl.

2.5. PCR

An initial screen of the DNA was performed using a broadly targeted anti-metazoan primer set (Bower et al. 2004) and a 'generic' *Neo/Paramoeba* primer set (Bojko et al. 2018) (Table 1). Having identified the amoeba sequences present in the sample as clustering with *N. pemaquidensis* and *N. aestuarina*, plus a novel paramoebid lineage, 4 nested primer sets were designed: 2 nested sets specific to the novel lineage: 210FA–1319R first round followed by 210FB–1319R (expected amplicon size ca. 1109 bp) and 210FA–1319R first round followed by 210FA–478R second round (expected amplicon size ca. 268 bp), and 2 nested sets targeting most of the known diversity of *Neo/Paramoeba* sequence types, including all *N. pemaquidensis* and *N. aestuarina* sequence types but excluding the novel lineage. Of these 2 sets, 56f–

Table 1. List of generic 18s primers used for the initial PCR screen of samples

Primer	Sequence (5′–3′)	Reference
18s-EUK581-F	GTG CCA GCA GCC GCG	Bower et al. (2004)
18s-EUK1134-R	CGC AAG GCT GAA ACT TAA A	Bower et al. (2004)
Amoeba F1	TAT GGT GAA TCA TGA TAA CTT WAC	Bojko et al. (2018)
Amoeba R1	TCT CCT TAC TAG ACT TTC AYK	
Amoeba F2	AAT CAT GAT AAC TTW ACG AAT CG	

1165R nested with 150F–1165R produced an amplicon of ca. 1 kb, and 56f–R1 nested with 150F–R1 produced an amplicon of ca. 630 bp. All primer sequences designed and used in this study are shown in Table 2. The primer set that amplified the short amplicon (210FA–478R) of the novel sequence, along with both of the generic primer sets were used to screen DNA extracted from heart, hepatopancreas and gill tissue from sample sets October 2019 (n = 30) and November 2019 (n = 22), and hepatopancreas and gill tissue from December 2020 (n = 46).

For the 2 nested generic PCRs (56F–1165R followed by 150F–1165R [long amplicon] and 56f–R1 followed by 150F–R1 [short amplicon]) and the novel lineage-specific long amplicon PCR (210FA–1319R followed by 210FB–1319R), the following thermocycling conditions were used for both first and second rounds: 95°C for 2 min; followed by 35 cycles of 95°C for 1 min, 60°C for 1 min and 72°C for 1 min; and a final extension at 72°C for 10 min. For the novel lineage-specific (short amplicon) PCR (210FA–1319R followed by 210FA–478R), the annealing temperature for both the first and second rounds was set at 63°C. The first-round PCR product was diluted 1/10 before being added to the nested PCR. PCR reactions were set up in a final volume of 25 µl with final concentrations of 1× Green GoTaq® Flexi Buffer (Promega), 1.5 mM $MgCl_2$, 0.2 mM dNTPs, 0.2 µM each of the forward and reverse primer, 1.25 units of GoTaq® G2 Flexi DNA Polymerase (Promega), 1.25 µl extracted nucleic acid and 15.92 µl molecular grade H_2O. Amplifications were performed on a Mastercycler® nexus (Eppendorf) thermal cycler with a 100°C-heated lid to prevent evaporation. Amplification products were resolved on 2% TBE agarose gels stained with Gel Red. Gels were run at 120 V for approximately 20 min and visualized using a UV illuminator. Correct-size products amplified using both primer sets were purified from PCR products using the Wizard® SV Gel and PCR Clean-Up System (Promega). Purified DNA positive for the novel lineage PCR was quantified using a Nanodrop (Thermo Scientific) and sent to Eurofins Genomics, Luxembourg, for sequencing. Purified DNA positive for the generic PCR was quantified using the Quanti-Fluor® dsDNA System on the Quantus™ Fluorometer (Promega) prior to cloning. Ligation and transformation were completed using pGEM®-T Easy Vector Systems (Promega) and JM109 competent cells (Promega) following the manufacturer's instructions. This was necessary because more than one amoeba lineage was present in some samples. White clones containing inserts were checked by colony PCR using specific primers. PCR products were then sequenced as described above. Subsequent analysis, checking the quality of the sequence and trimming of unreadable chromatogram peaks, was completed using Bioedit 7.2.5 (Hall 1999) and CLC main Workbench 21. Sequences were then matched against the National Center for Biotechnology Information (NCBI) nucleotide database using the Basic Local Alignment Search Tool (BLASTn).

Table 2. List of specific primers designed in this study to amplify both novel (*Janickina feisti*-specific) and generic paramoebae found. ISH: *in situ* hybridisation

Primer	Sequence (5′–3′)
210FA: *J. feisti*-specific	TAA CTT TAC GAA TCG CAC ACT T
210FB: *J. feisti*-specific	CGA ATC GCA CAC TTA TGA TAT AC
1319R: *J. feisti*-specific	CTG TCA ATC CTA ACT GTG TCT G
478R: *J. feisti*-specific	CCA GAA CTT GCC CTC GAA TC
S19probeF: *J. feisti*-specific ISH	CGA AGA GAT AAC ATA TAA ACC
S19probeR: *J. feisti*-specific ISH	CTA ATA GTA TTC ATT GCT TAA ATT C
56F	ATT TGA TGG TCT TTT ACT ACT TGG
1165R	CGT AAG GTR CTG AAG GAG TTT
150F	TTA GAT TCA AAA GCC AAT GCC A
R1	TCT CCT TAC TAG ACT TTC AYS

2.6. *In situ* hybridisation (ISH)

A digoxygenin (DIG)-labelled DNA probe was synthesised using the s19probeF–s19probeR primer set (Table 2) to produce an 18S-targeted probe specific to the novel paramoebid lineage. The probe was synthesised by PCR in 100 µl volume reactions with a final concentration of 1× Green GoTaq® Flexi Buffer (Promega), 2.5 mM $MgCl_2$ (Promega), 1× PCR DIG labelling mix (Roche Applied Science), 2.5 u GoTaq® G2 Flexi DNA polymerase (Promega), 0.5 µM forward primer, 0.5 µM reverse primer, 0.01 mg ml^{-1} BSA (New England Bioscience) and 6 µl template DNA. Cycling conditions were as follows: 94°C for 5 min; followed by 35 cycles of 94°C for 1 min, 50°C for 1 min and 72°C for 1 min; with a final extension of 72°C for 10 min.

ISH was carried out using an adaption of the methods described by Montagnani et al. (2001) and Fabioux et al. (2004). Sections of gill, hepatopancreas, heart, muscle and gonad were collected onto poly-L-lysine-coated glass slides from animals that were (1) PCR

positive for the novel paramoebid lineage (samples Oct19-1,9,19,30; Table S1 in the Supplement at www.int-res.com/articles/suppl/d150p001_supp.pdf), 3 of which were PCR negative for *N. pemaquidensis*/*N. aestuarina*, and (2) PCR negative for the novel lineage but PCR positive for *N. pemaquidensis*/*N. aestuarina* (samples Dec20-35,36; Table S1). Sections were dewaxed in xylene substitute (Thermo Scientific) 2 times for 5 min and rehydrated in 100% industrial denatured alcohol (ethyl alcohol solution, Pioneer Research Chemicals) twice for 5 min. Sections were treated with Proteinase K (Sigma Aldrich) (100 µg ml^{-1}) at 37°C for 15 min in a humid chamber before dehydration in 100% IMS for 5 min. Slides were rinsed with 2× SSC (Sigma Aldrich) and hybridised overnight at 40°C with 125 µl of DIG-labelled probe diluted 1:1 with hybridisation buffer (4× SSC, 50% formamide [VWR], 1× Denhardt's solution [Invitrogen], 250 µg ml^{-1} yeast tRNA [Thermo Scientific], 10% dextran sulphate [Millipore]). Negative control slides (one corresponding to each slide hybridised with probe) were incubated with hybridisation buffer with the exclusion of DIG-labelled probe. Slides were washed with 2× washing buffer (2× SSC, 6 M urea, 2 mg l^{-1} BSA) 2 times for 15 min at 40°C. Endogenous phosphate activity was blocked by incubation in 6% skimmed milk (Sigma Aldrich) in Tris 7.5 buffer (0.15 M NaCl, 0.1 M Tris base, pH 7.5) for 1 h, prior to incubation with anti-DIG-AP, Fab fragments (Roche Applied Science), diluted 1:300 with Tris 7.5 buffer for 1 h. Slides were washed with Tris 7.5 buffer 5 times for 5 min followed by washing with Tris 9.5 buffer (0.1 M NaCl, 0.1 M Tris base, pH 9.5) for 20 s. The hybridisation signal was detected using nitroblue tetrazolium/5-bromo-4-chloro-3-indolyl phosphate (Roche Applied Science) diluted 20 µl ml^{-1} in Tris 9.5 buffer for 10 min. Slides were washed with Tris 9.5 buffer for 2 min and counterstained with Nuclear Fast Red solution (Sigma Aldrich).

2.7. Phylogenetics

Phylogenetic trees were built with MrBayes v.3.2.6 (Ronquist et al. 2012). Two separate MC^3 runs with randomly generated starting trees were carried out for 5 million generations each with 1 cold and 3 heated chains. The evolutionary model applied a GTR substitution matrix, with a 4-category autocorrelated gamma correction and the covarion model. All parameters were estimated from the data. The trees were sampled every 1000 generations, and the first 1.25 million generations were discarded as burn-in. All phylogenetic analyses were carried out on the CIPRES server (Miller et al. 2010).

3. RESULTS

3.1. Macroscopic findings

Prior to dissection, some crabs (16%) were noted to be lethargic and slow to respond to stimuli, other crabs appeared to be healthy and responsive. Upon dissection, the connective tissues of the lethargic crabs appeared spongy and of a watery consistency; in non-lethargic crabs, melanised nodules (granuloma) were observed in the hepatopancreas and heart.

3.2. Histology

Histopathology revealed a significant host cellular response in the majority of crabs (62%), with pronounced haemocytic infiltration leading to congestion of haemal spaces, particularly within the hepatopancreas and at locations where otherwise large haemal lacunae would be expected (Fig. 1A). In some individuals, masses of an amoeboid parasite occurred within the haemal sinuses, fixed phagocytes (Fig. 1C) and apparently within connective tissue cells of the heart (Fig. 1D) and gills (Fig. 1E). Amoeba-like cells appeared to be the focus of these haemocyte accumulations, suggesting recognition of parasite cells by host haemocytes. Amoebae were spherical to elongate in shape and measured 4–12 µm in length and 4–9 µm in width (n = 60). In most cases, 2 clearly visible nuclei were observed within these cells (Fig. 1B), leading to a presumptive diagnosis of infection by a *Paramoeba*-like pathogen using light microscopy. Some crabs displayed large numbers of amoeba-like cells within remnants of fixed phagocyte clusters in the hepatopancreas and within connective tissue cells of the hepatopancreas, heart and gills. Melanised host reactions were occasionally observed in the gills (Fig. 1F) and heart. We did not observe any other infections or co-infections in tissue sections from crabs sampled from these sites.

3.3. TEM

Electron microscopy confirmed the presence of an amoeba-like pathogen in the tissues of crabs previously identified as being infected via histology. TEM confirmed the presence of a single apparent *Per-*

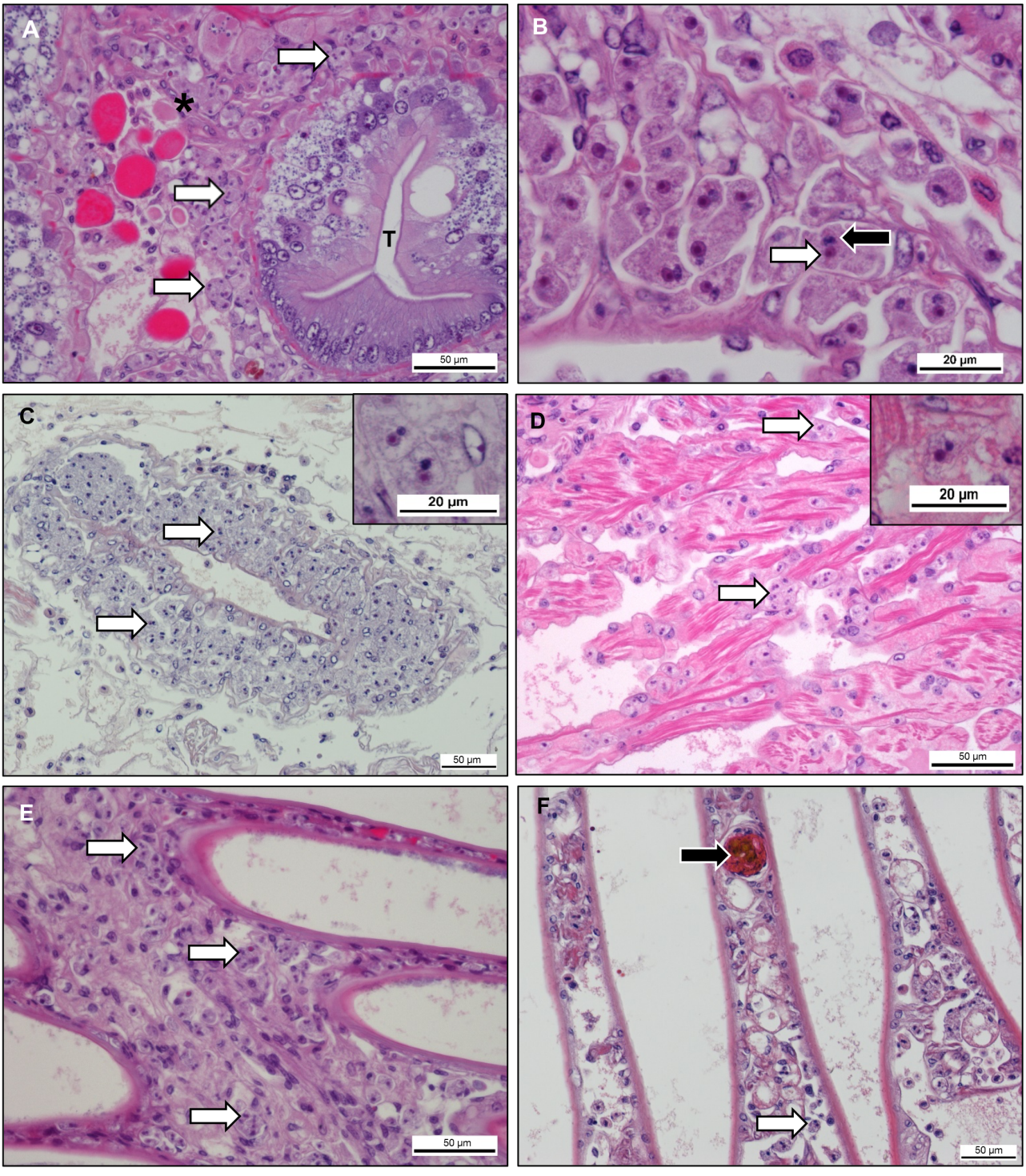

Fig. 1. *Janickina feisti* within tissues of edible crab. (A) Haemal sinuses (*) between the hepatopancreas tubules (T) appeared congested with host haemocytes; clear paramoeba cells (arrows) can be seen distributed throughout the host response. (B) Paramoebae distributed throughout the haemal sinuses between the hepatopancreas tubules appear to contain a nucleus (white arrow) with clear nucleolus and a *Perkinsela*-like organism (PLO) (black arrow). (C) Paramoebae infected the fixed phagocytes in heavy infections; paramoebae identified within the exterior cells of the arteriole (arrows). Inset: paramoeba cells containing clear nucleus and PLO. (D) Paramoebae (arrows) within connective tissues of the heart in heavily infected crab. Inset: paramoeba cells containing clear nucleus and PLO. (E) Paramoebae (arrows) within haemal spaces of the gill lamellae. (F) Melanised host reaction (black arrow) and paramoeba (white arrow) within the gill lamellae. All images: H&E stain

kinsela-like endosymbiont in close association with the amoeboid nuclei of most cells (Fig. 2A,D). The *Perkinsela*-like organism appeared spherical in shape and measured 1–3 µm in diameter. Amoebae contained numerous mitochondria, vacuoles, a Golgi body, electron dense vesicles and electron lucent vesicles distributed throughout the cytoplasm (Fig. 2B,C). Pseudopodia-like structures were observed projecting from the peripheral cell membrane in some cases (Fig. 2A). Amoeba cells were ovoid to elongate in shape and measured 6–16 µm in length and 3–10 µm in width (n = 10). The outer membrane was distinctive in appearance, with some areas appearing crenulated; electron lucent vesicles were seen lining the cell membrane, potentially indicating sites of pinocytosis/exocytosis (Fig. 2E,F). No scale-like structures were observed on the membrane of amoeba cells. However, a glycocalyx-like layer was observed on the outermost surface; hair-like structures (glycostyles) were observed within this layer and measured approximately 55 nm in length. The glycocalyx layer and hair-like structures were also observed on the internal surface of the electron lucent vesicles within the cytoplasm (Fig. 2F).

3.4. ISH

ISH labelling with a probe designed to be specific to the novel paramoebid lineage revealed densely stained cells in the arterioles (Fig. 3B), haemal sinuses of the hepatopancreas (Fig. 3D) and gill tissues (Fig. 3F). Cells corresponding to those previously identified as an amoeboid parasite and associated with pathology in H&E-stained sections were shown to stain a deep blue colour, highlighting positive labelling with the novel lineage-specific probe, in all 4 samples that were PCR-positive for the novel lineage. No labelling was observed in negative control tissue sections (Fig. 3A,C,E). The probe was also applied to tissue sections from crabs which were strongly PCR positive for *N. aestuarina* and *N. pemaquidensis* but PCR negative for the novel lineage; no labelling was observed in any of these tissue sections. Furthermore, amoeba cells were not observed by histology in tissues of any of the crabs which were PCR positive for *N. aestuarina*/*N. pemaquidensis* but not for the novel lineage.

3.5. PCR and sequence analysis

The anti-metazoan and generic *Neo*/*Paramoeba* PCRs amplified 6 lineages that grouped with *N. pemaquidensis* and *N. aestuarina* sequences in preliminary phylogenetic trees (not shown), and a novel, divergent sequence distinct from any known paramoebid, but still branching in the paramoebid clade, robustly sister to, but genetically highly distinct from, *Janickina pigmentifera*. Based on these initial sequence data, primer sets were designed to produce longer amplicons for increased phylogenetic and taxonomic resolution, and to provide more accurate targeting/screening of the novel lineage and the other sequence types in the *N. pemaquidensis* and *N. aestuarina* radiation.

Table 3 shows the results of PCR screens using the nested PCR protocols specific to the novel amoeba, the *Neo*/*Paramoeba* targeted primer set producing the longest amplicon (56F–1165R/150F–1165R), and a summary of the corresponding histopathology results. Very faint PCR positives (indicated by '+' in Table S1) were not counted as positive results in the total summarised in Table 3, or as presented below.

The novel amoeba was detected by PCR in all of the samples in which amoeba cells were observed by histology (24/24; Table S1). In contrast, only 10 of the 24 samples in which amoebae were observed by histology were PCR positive for *N. pemaquidensis* and *N. aestuarina*, and all of these were PCR positive for the novel amoeba. Similarly, the novel amoeba was detected by PCR in all samples in which host response was observed, with the exception of the December 2020 sample set, in which only 16 of the 31 samples showing host response were PCR positive for the novel amoeba. Samples in which host response was observed (n = 61) also corresponded more strongly with positive PCR results for the novel amoeba than for *N. pemaquidensis* and *N. aestuarina*: 46/61 positive PCR results for the novel amoeba and 31/61 for *N. pemaquidensis*/*N. aestuarina*. There was complete correspondence between novel amoeba PCR positives and host response for the October and November 2019 sample sets, but not for December 2020 (Table 3; Table S1). The novel amoeba was detected by PCR far more frequently in heart tissues than the other lineages (27/52 vs. 3/52).

Amoeba cells were not observed by histology (or ISH) in histological sections of any samples which were PCR positive for *N. aestuarina*/*N. pemaquidensis* but negative for the novel lineage (a total of 20 samples; Table S1). There were no histological observations of amoebae in samples PCR negative for all amoeba lineages (n = 24), although 7 of these showed a host response, but only in the December 2020 set. Of the 36 samples across all sampling points in which no infecting amoebae or host responses were ob-

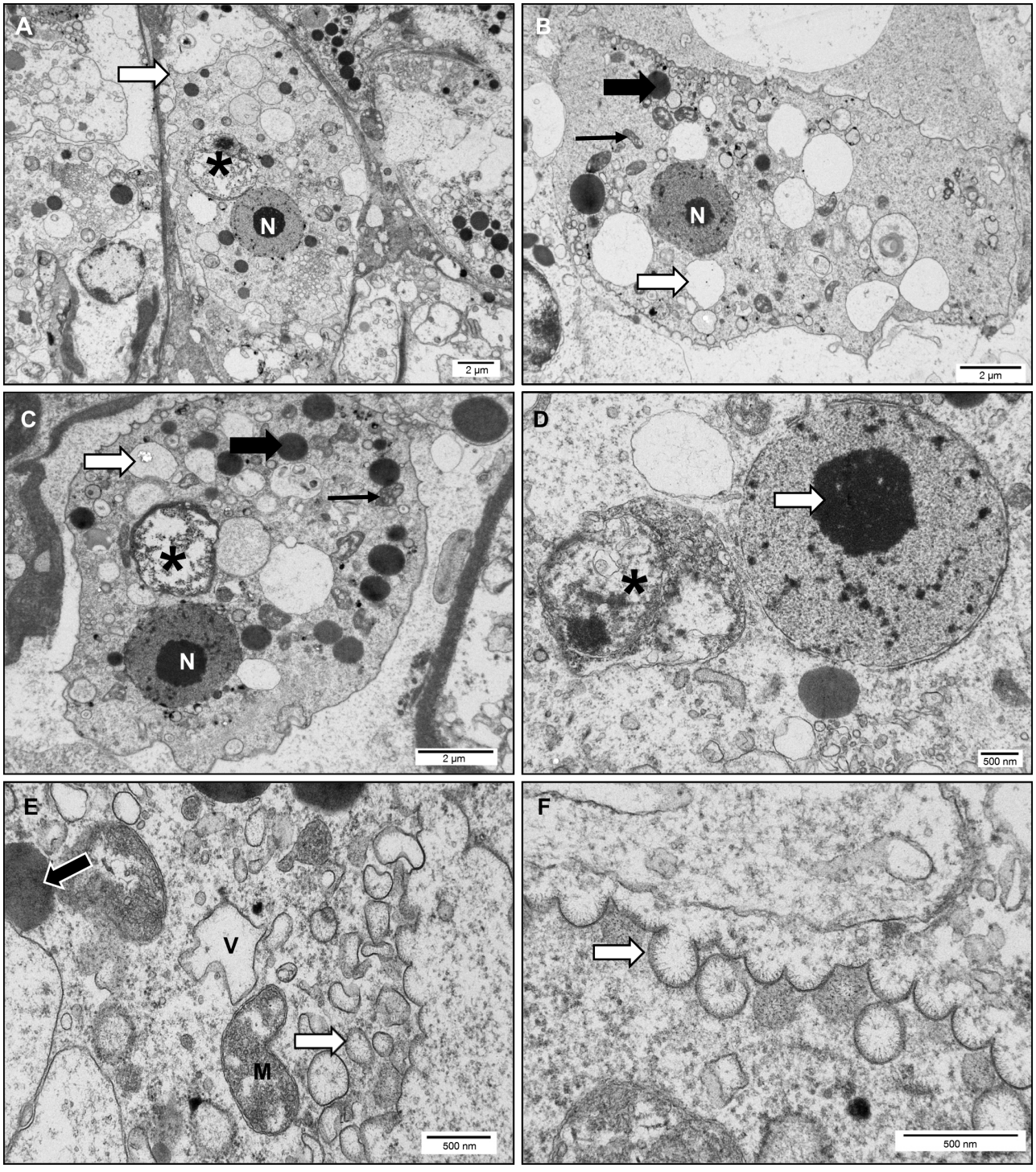

Fig. 2. *Janickina feisti* within tissues of edible crab. (A) *Paramoeba* showing a clear nucleus (N) and endosymbiont *Perkinsela* sp. (*), with pseudopodia-like structures at the peripheral membrane (arrow). (B) Amoeba with clear nucleus (N), mitochondria (line arrow), electron dense vesicles (black arrow) and electron lucent vacuoles (white arrow) distributed throughout the cytoplasm. (C) Amoeba showing a clear nucleus (N) and endosymbiont *Perkinsela* sp. (*), mitochondria (line arrow), electron dense vesicles (black arrow) and electron lucent vacuoles (white arrow) distributed throughout the cytoplasm. (D) Nuclei within the amoeba display prominent nucleolus (white arrow) and show close association with the endosymbiont *Perkinsela* sp. (*). (E) Cytoplasmic organelles within paramoeba, mitochondria (M), vacuole (V), electron dense (black arrow) and lucent (white arrow) vesicles. (F) Higher magnification image of cell membrane and exchange of materials via pinocytosis/exocytosis (arrow). Electron lucent vacuoles appear to line up along the crenulated external cell membrane of the paramoeba

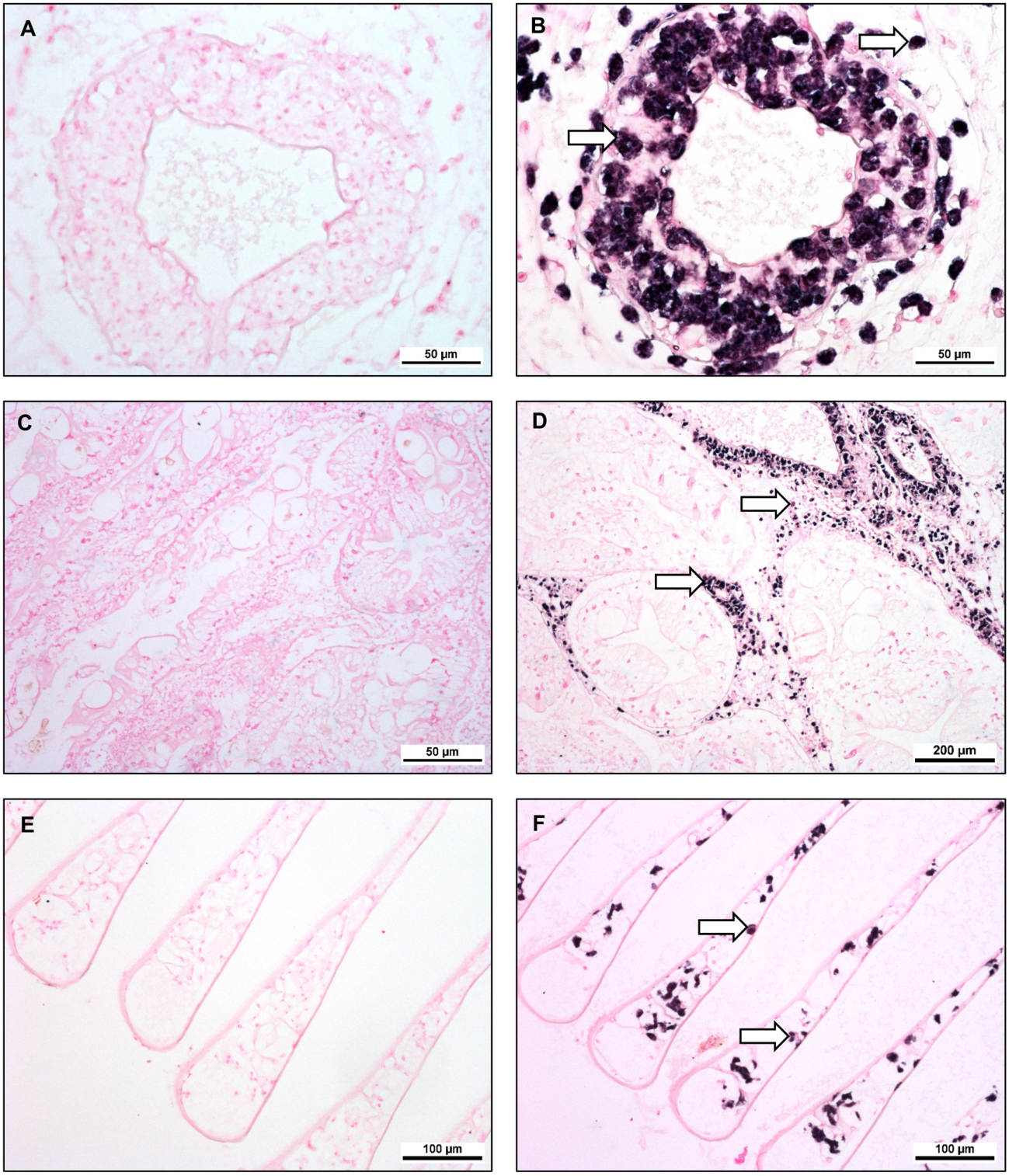

Fig. 3. *In situ* hybridisation (ISH) of tissues of edible crab. (A) Negative control section of an arteriole; note the lack of labelling. (B) ISH of a similar region of tissue in closely adjacent section using *Janickina feisti* probe. Note the presence of densely stained (positively labelled) *J. feisti* cells (arrows). (C) Negative control section of the hepatopancreas, no labelling was observed. (D) ISH-labelled section of hepatopancreas. Note the presence of positively labelled *J. feisti* cells in the haemal sinuses (arrows). (E) Negative control section of gill tissues, no labelling was observed. (F) ISH-labelled section of gill. *J. feisti* cells are clearly labelled with the dense stain (arrows)

Table 3. Comparison of molecular and histological data highlighting where the detection of the novel *Janickina* species (*J. feisti*) and *Neoparamoeba pemaquidensis* and *N. aestuarina* via PCR corresponded to detection of amoeba-like cells and pathology within the crab tissues. The full dataset, with results for each crab individual, is shown in Table S1. PCR positives here exclude the very weak positives indicated by '+' in Table S1

Sample	*J. feisti* PCR-positive			*N. pemaquidensis* and *N. aestuarina* PCR-positive			Histology (% of histology-positive samples also PCR-positive for *J. feisti*, other paramoebae)	
	Gill	Hepato-pancreas	Heart	Gill	Hepato-pancreas	Heart	Amoeboid cells observed	Host response observed
October 2019	24/30	12/30	24/30	8/30	4/30	2/30	18/30 (100, 33)	24/30 (100, 42)
November 2019	6/22	3/22	3/22	9/22	1/22	1/22	5/22 (100, 60)	6/22 (100, 67)
December 2020	19/46	10/46	n.d.	26/46	6/46	n.d.	1/46 (100, 100)	31/46 (52, 55)

served, 7 were PCR positive for the novel amoeba and 15 were positive for *N. pemaquidensis* and *N. aestuarina* (Table S1).

Sequences generated in this study were submitted to GenBank (*Neoparamoeba aesturina*: MZ773583–MZ773603; *N. pemaquidensis:* MZ773561–MZ7735 82; *J. feisti*: MZ773604).

3.6. Phylogenetic analyses

Fig. 4 is a Bayesian phylogenetic analysis summarising the branching position of the cloned sequences from different tissue samples from individual crabs. The branches are shown collapsed, as there is small-scale sequence variation within most paramoebid species. An un-collapsed version of the tree is shown in Fig. S1

The analysis showed that 22 sequence types branched with existing *N. pemaquidensis* sequences (Clade A in Fig. 4), in 2 main clusters (Fig. S1), both also including previously published sequences from salmonid fish and aquaculture sites. All but 1 of the 21 *N. aestuarina* clones clustered together to the exclusion of all other known sequence types from that species, having at least 3% 18S sequence difference from sequences in GenBank; these are labelled as 'novel *C. pagurus* clade' in Fig. S1. The single other *N. aestuarina* clone branched in Clade C (Fig. 4).

The majority of the *N. pemaquidensis* clones were derived from gill samples, with the remaining sequences derived from a hepatopancreas sample from a single individual (Table 3; Table S1). Similarly, only 1 *N. aestuarina* sequence did not derive from gill samples and did not group in the novel *N. aestuarina* clade, which comprised only sequences from gill samples (Table 3; Fig. S1, Table S1).

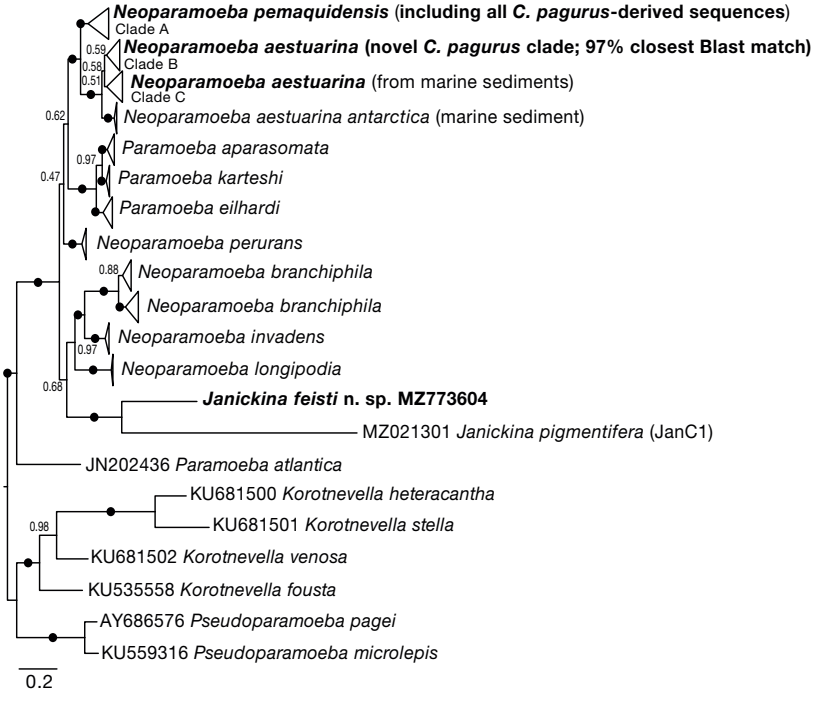

Fig. 4. 18S rRNA gene Bayesian phylogeny of all known paramoebid lineages for which 18S sequence data are available, including the new species described in this paper, *Janickina feisti*. Sequences generated in this study are indicated by **bold** text. Collapsed branches comprise clades of closely related sequences corresponding to individual species or subclades within species. A non-collapsed version of this tree is shown in Fig. S1. Bayesian posterior probability (BPP) values are indicated at each node; filled black circles represent full BPP support (BPP = 1) for the node indicated

The novel amoeba 18S sequence branched with full Bayesian posterior probability support as sister to *J. pigmentifera* (Fig. 4). The phylogenetic position of the *Janickina* branch was not resolved within the paramoebid clade, but the 2 *Janickina* sequences are strongly mutually related and very distinct from all other paramoebids.

3.7. Historic data analysis

Data from previous edible crab health surveys conducted at Cefas between 2002 and 2021 (Stentiford et al. 2002, 2003, 2007, Bateman & Stentiford 2008, Feist et al. 2009, Bateman et al. 2011, 2016, Hartikainen et al. 2014) were re-evaluated to determine whether pathologies like those described here were present. A total of 620 edible crabs sampled directly from fisheries in the English Channel and 2860 juvenile edible crabs collected from the shoreline at 4 separate sites around the coast of England and Wales were examined over this period. None of these samples reported histological evidence of a paramoebid infection or associated pathologies consistent with paramoebiasis within the tissues.

4. DISCUSSION

We provide the first report of paramoebiasis in edible crabs and name this condition amoebic crab disease (ACD). Although we have no data on the presence and prevalence of ACD beyond the immediate location sampled, we can confirm that the agent(s) implicated in this disease have not previously been detected in extensive studies of adult and juvenile crabs collected from multiple locations in the English Channel, North Sea and Irish Sea by our and other laboratories over at least the past 20 yr. Additionally, the 18S rRNA gene sequence of the novel lineage is highly distinct from any previously reported paramoebid sequence.

Amoeboid cells, predominantly or exclusively the novel lineage, were observed by histology distributed throughout multiple tissues (gills, heart, fixed phagocytes, haemal sinuses), in particular the connective tissues and haemal spaces of the hepatopancreas. Significant host immune response was evident in some individuals with pronounced haemocytic infiltration and aggregations of phagocytes congesting the haemal spaces. The pathology observed in heavy infections is considered sufficient to lead to morbidity and mortality in crabs. Histologically, the infection appears very similar to grey crab disease described previously in blue crabs (Johnson 1977); however, no external sign of infection was noted in the individuals sampled in this study, apart from lethargy.

In blue crabs, the midgut epithelium was suggested to be a logical portal of entry for the amoebae due to high numbers, present in connective tissues surrounding the gut and the higher likelihood of amoebae in these areas in light infections (Johnson 1977). Johnson (1977) had reported small (3–7 µm) and large forms (10–25 µm) of the parasite; large forms were observed in the antennal gland and nervous system. Unlike grey crab disease, we did not observe 2 cell types in ACD. We observed a range of spherical to elongate cells measuring 4–12 µm in length and 4–9 µm in width distributed throughout edible crab tissues. Johnson (1977) suggested that infection of heart tissues in blue crabs was an artefact of sampling; here we clearly show infection of the connective tissue cells in the heart of edible crabs. *Paramoeba perniciosa* is not formally recognised as a *Paramoeba* species, as species characterisation was based upon morphology alone and no genetic information is available for comparison; however, it has been suggested that *P. perniciosa* may be conspecific with other well characterised amoebae (English & Lima 2020).

TEM observations of the novel parasite supported the presumptive diagnosis from light microscopy. The amoeboid cells were confirmed to possess a *Perkinsela*-like organism, an intracellular endosymbiont characteristic of the *Neo/Paramoeba* (Dyková et al. 2003). Amoeboid cells observed in this study contained a single *Perkinsela*-like organism in close association with the amoeboid cell nuclei. No scales were observed on the outer membrane of the amoeboid cells; instead, we observed a glycocalyx layer covering the external surface of the cell membrane. Hair-like projections occurred in this layer, regularly distributed along the membrane. It has been suggested that the presence of this glycocalyx layer may be an adaptation to parasitism, with the composition of the layer shown to vary between parasitic and non-parasitic forms of some *Paramoeba* species (Nowak & Archibald 2018). *Janickina pigmentifera* is covered in a layer of a stratified glycocalyx that differs from the cell coat of *Neoparamoeba* and *Paramoeba*. *J. pigmentifera* is an obligate parasite which infects the testes of marine arrow worms, and it has been suggested that its distinct morphology compared to *Neo/Paramoeba* is related to its obligate parasitic lifestyle (Volkova & Kudryavstev 2021).

In some regions of the amoeboid cell membrane of the novel parasite, crenulation occurred, corresponding with the presence of electron lucent vesicles. We observed a glycocalyx layer with hair-like projections on the internal membrane of these electron lucent vesicles. The vesicles aligned on the inner membrane, presumably for exchange of materials between the amoeboid cells and host tissues. Other paramoebid species are reported to be much larger in size and either lack or possess multiple *Perkinsela*-like organisms, and some possess scale-like structures on their cell membranes. Compared to other species, the novel amoeba is similar in size and shape to *P. perniciosa* described as the agent of grey crab disease in blue crabs, with both species reported to contain a single *Perkinsela*-like organism. TEM and molecular data are not available for *P. perniciosa* to enable fine comparison of surface structure between these species, or to determine the phylogenetic position of *P. perniciosa*.

Morphology alone is an unreliable tool for species identification given the diversity in amoeba size and shape within a species, and it is noted that different species and even genera are often indistinguishable at the light microscope level (Nowak & Archibald 2018, English & Lima 2020). During our investigation, unsuccessful attempts were made to culture the novel amoeba (data not shown); therefore, we describe its structural features based upon fixed tissues only. It should thus be noted that some of the morphological and dimensional observations provided here may differ from cells in wet preparations.

Although we were unable to make direct morphological comparisons between the novel amoeba and *Janickina* species as provided and summarised by Volkova & Kudryavstev (2021), the phylogenetic position of the 18S sequence of the novel crab-infecting amoeba was sister to *J. pigmentifera* with maximal support. The morphology of our novel amoeba is consistent with that of *Janickina* spp., as far as we can determine, and similarly appears to be an obligate parasite. Therefore we formally describe the crab-infecting amoeba as a novel species of *Janickina*, *J. feisti*, in the taxonomic summary below (Section 5).

In addition to the identification of *J. feisti,* we identified a range of *Neoparamoeba* lineages associated with the pathology, although in most cases pathology was only associated with the molecular detection of *J. feisti*. The small number of samples which were PCR-positive for *J. feisti* but showed no histopathology could be explained by the fact that a larger volume (and different section) of tissue was interrogated by the molecular assays than via histology, and therefore the molecular approach may have more opportunity to detect localised infection. Further, the nested PCR protocol would likely detect low-level infections that are not easily visible by histological screening. The weaker association between PCR-positive results for the novel amoeba and host response in the December 2020 sample set is worthy of further investigation and may be explained by less recent infection by *J. feisti* in this set compared to the other two; this would also account for the very low level of histological observations of infecting amoeba in this sample set.

The association between PCR detection of *N. pemaquidensis* and *N. aestuarina* and visible amoeba cells and/or host response was far weaker than for *J. feisti*. No amoeba cells were observed via histology in any tissues from samples which were PCR positive for *N. aestuarina* and *N. pemaquidensis* but PCR negative for *J. feisti*. However, in some cases strong PCR positives of all paramoebid lineages coincided with infection/pathology; in these cases, it is possible that *N. pemaquidensis/aestuarina* were contributing to the pathological manifestation of ACD, although we can provide no evidence that this was the case. The fact that samples strongly PCR-positive for *N. pemaquidensis/aestuarina* were either positive for *J. feisti*, or had no infection/pathology noted, and were largely associated with tissues either exposed to the external environment (gill), part of the digestive system (hepatopancreas), but very rarely (by PCR) heart tissue (which is part of the closed circulation system), suggests that PCR detection of *N. pemaquidensis/aestuarina* may represent incidental or secondary infections, or opportunist colonizers from the surrounding environment. The high incidence of weak *N. pemaquidensis/aestuarina* PCR positives distributed across all sample types is consistent with this hypothesis, as is the similarity of our *N. pemaquidensis/aestuarina* sequences to many others from a range of marine environments present in GenBank. In contrast, the *J. feisti* sequence has never previously been recorded from any sample type or associated with any host.

Despite potential for involvement by other paramoebids, we propose that *J. feisti* is the main causative agent of ACD. However, in the December 2020 sample set, 8/46 animals showed pathology associated with strong PCR detection of *N. pemaquidensis/aestuarina* whilst negative for *J. feisti*. Therefore, further studies are required to investigate what may potentially be a pathobiotic system (Bass et al. 2019, Bass & del Campo 2020), involving multiple agents. If so, ACD may have parallels with amoebic gill disease

(AGD) in salmonids. The causative agent of AGD has been identified as *N. perurans*, but this disease is often associated with a range of amoeba species (English et al. 2019a,b), whose role in AGD aetiology remains unclear. For example, *N. pemaquidensis* and *N. branchiphila* have been isolated from AGD-affected fish but experimental exposure of fish to these species did not result in AGD (Nowak & Archibald 2018). The detailed aetiology of ACD remains to be determined, but we provide strong evidence for a causative role of the newly discovered *J. feisti*. So far *J. feisti* has only been detected at the English Channel site, and its possible distribution in edible crabs more widely and in other sample types (water, sediment, other hosts) is currently under investigation. Further studies are required to investigate the potential role of ACD as a mortality driver in commercially exploited populations of *C. pagurus* in European waters.

5. TAXONOMIC SUMMARY

Diagnosis of *Janickina feisti*

Position in the system according to Adl et al. (2019): Amorphea: Amoebozoa: Discosea: Flabellinia: Dactylopodida
Genus: *Janickina* Grassi, 1896
Species: *Janickina feisti* sp. nov. Bateman et al. 2022
Diagnosis: Spherical to elongate cells which when observed histologically appear to contain 2 nuclei. Cells contain a single intracellular endosymbiont, a *Perkinsela*-like organism. Cells measure 4–16 µm in length and 3–9 µm in width, can be seen distributed throughout the connective tissues, fixed phagocytes and haemal spaces in the gill, heart and hepatopancreas tissues. Cells are associated with intense host (*Cancer pagurus*) response with extensive haemocytic infiltration and congestion of haemal spaces in advanced infections.
Type host: Edible/brown crab *Cancer pagurus*
Type locality: English Channel, 2.5–3 miles (4–4.8 km) off the coast of Selsey Bill, within ICES Sub Rectangle 30E9
Etymology: Specific epithet *feisti*: named in recognition of the great contribution of Professor Stephen W. Feist to parasitology and pathology of aquatic animals
Type material: Original slides used for this paper are stored together with biological material embedded in wax and epoxy resin in the Registry of Aquatic Pathology (RAP) at the Cefas Weymouth Laboratory. The type material is stored as PM38845 (specimen 19) and the type 18S rRNA gene sequence is deposited in GenBank under accession number MZ773604.

Acknowledgements. The work was supported by funding from the UK Department of Environment, Food and Rural Affairs (Defra) under contracts FA001, FB002, FC1215, FX001 and FX003. We thank Jonathan Hulland, Jason Mewett, Niall O'Rahelly, Tamsin Cochrane-Dyet and Jerry Skillman from the Fish Health Inspectorate for their assistance with sampling, and David Stone for assistance with molecular analyses.

LITERATURE CITED

Adl SM, Bass D, Lane CE, Lukeš J and others (2019) Revisions to the classification, nomenclature, and diversity of eukaryotes. J Eukaryot Microbiol 66:4–119
Bass D, del Campo J (2020) Microeukaryotes in animal and plant microbiomes: ecologies of disease? Eur J Protistol 76:125719
Bass D, Stentiford GD, Wang HC, Koskella B, Tyler CR (2019) The pathobiome in animal and plant diseases. Trends Ecol Evol 34:996–1008
Bateman KS, Stentiford GD (2008) *Cancer pagurus* bacilliform virus (*Cp*BV) infecting juvenile European edible crabs *C. pagurus* from UK waters. Dis Aquat Org 79: 147–151
Bateman KS, Hicks RJ, Stentiford GD (2011) Disease profiles differ between non-fished and fished populations of edible crab (*Cancer pagurus*) from a major commercial fishery. ICES J Mar Sci 68:2044–2052
Bateman KS, Wiredu-Boakye D, Kerr R, Williams BAP, Stentiford GD (2016) Single and multigene phylogeny of *Hepatospora* (Microsporidia) — a generalist pathogen of farmed and wild crustacean hosts. Parasitology 143: 971–982
Bojko J, Stebbing PD, Dunn AM, Bateman KS and others (2018) Green crab *Carcinus maenas* symbiont profiles along a North Atlantic invasion route. Dis Aquat Org 128:147–168
Bonami JR, Zhang S (2011) Viral diseases in commercially exploited crabs: a review. J Invertebr Pathol 106:6–17
Boschma H (1955) The described species of the family Sacculinidae. Zool Verh 27:1–76
Bower SM, McGladdery SE, Price IM (1994) Synopsis of infectious diseases and parasites of commercially exploited shellfish. Annu Rev Fish Dis 4:1–199
Bower SM, Carnegie RB, Goh B, Jones SRM, Lowe GJ, Mak MWS (2004) Preferential PCR amplification of parasitic protistan small subunit rDNA from metazoan tissues. J Eukaryot Microbiol 51:325–332
Chatton E (1953) Classe des Lobosa Leidy, 1879. Ordre des Amoebiens nus ou Amoebaea. In: Grassé PP (ed) Traité de Zoologie, Vol 1, Fasc II. Masson et Cie, Paris, p 42–46
Corbel V, Coste F, Bonami JR (2003) *Cp*SBV, a systemic virus of the edible crab, *Cancer pagurus* (L.). J Fish Dis 26:121–126
De Faria JG, Da Cunha AM, Pinto C (1922) Estudos sobre Protozoarios do mar. Mem Inst Oswaldo Cruz 15: 101–115

Dyková I, Fiala I, Lom J, Lukeš J (2003) *Perkinsiella amoebae*-like endosymbionts of *Neoparamoeba* spp., relatives of the kinetoplastid *Ichthyobodo*. Eur J Protistol 39:37–52

Dyková I, Nowak BF, Crosbie PBB, Fiala I and others (2005) *Neoparamoeba branchiphila* n. sp., and related species of the genus *Neoparamoeba* Page, 1987: morphological and molecular characterization of selected strains. J Fish Dis 28:49–64

English CJ, Lima PC (2020) Defining the aetiology of amoebic diseases of aquatic animals: trends, hurdles and best practices. Dis Aquat Org 142:125–143

English CJ, Swords F, Downes JK, Ruane NM and others (2019a) Prevalence of six amoeba species colonising the gills of farmed Atlantic salmon with amoebic gill disease (AGD) using qPCR. Aquacult Environ Interact 11: 405–415

English CJ, Tyml T, Botwright NA, Barnes AC, Wynne JW, Lima PC, Cook MT (2019b) A diversity of amoebae colonise the gills of farmed Atlantic salmon (*Salmo salar*) with amoebic gill disease (AGD). Eur J Protistol 67:27–45

Fabioux C, Huvet A, Lelong C, Robert R and others (2004) Oyster *vasa*-like gene as a marker of the germline cell development in *Crassostrea gigas*. Biochem Biophys Res Commun 320:592–598

Feehan CJ, Johnson-Mackinnon J, Scheibling RE, Lauzon-Guay JS, Simpson AGB (2013) Validating the identity of *Paramoeba invadens*, the causative agent of recurrent mass mortality of sea urchins in Nova Scotia, Canada. Dis Aquat Org 103:209–227

Feist SW, Hine PM, Bateman KS, Stentiford GD, Longshaw M (2009) *Paramarteilia canceri* sp. n. (Cercozoa) in the European edible crab (*Cancer pagurus*) with a proposal for the revision of the order Paramyxida Chatton, 1911. Folia Parasitol 56:73–85

Grassi B (1881) Intorno ai chetognati. R Ist Lombardo Sci e Lett 2:185–224

Grell KG, Benwitz G (1970) Ultrastruktur mariner Amöben 1. *Paramoeba eilhardi* Schaudinn. Arch Protistenkd 112: 119–137

Hall TA (1999) BioEdit: a user-friendly biological sequence alignment editor and analysis program for Windows 95/98/NT. Nucleic Acids Symp Ser 41:95–98

Han JE (2019) Detection of the amoebic parasite (order Dactylopodida) in cultured Pacific white shrimp (*Litopenaeus vannamei*) Aquaculture 507:246–250

Hartikainen H, Stentiford GD, Bateman KS, Berney C and others (2014) Mikrocytids are a broadly distributed and divergent radiation of parasites in aquatic invertebrates. Curr Biol 24:807–812

Janicki C (1912) Untersuchungen an parasitischen Arten der Gattung *Paramoeba* Schaudinn (*P. pigmentifera* Grassi und *P. chaetognathi* Grassi.). Verh Naturforsch Ges Basel 23:6–21

Johnson PT (1977) Paramoebiasis in the blue crab, *Callinectes sapidus*. J Invertebr Pathol 29:308–320

Jones GM (1985) *Paramoeba invadens* n. sp. (Amoebida, Paramoebidae), a pathogenic amoeba from the sea urchin, *Strongylocentrotus droebachiensis*, in eastern Canada. J Protozool 32:564–569

Kudryavtsev A, Pawlowski J, Hausmann K (2011) Description of *Paramoeba atlantica* n. sp. (Amoebozoa, Dactylopodida) — a marine amoeba from the Eastern Atlantic, with emendation of the dactylopodid families. Acta Protozool 50:239–253

Kudryavtsev A, Volkova E, Voytinsky F (2021) A checklist of Amoebozoa species from marine and brackish-water biotopes with notes on taxonomy, species concept and distribution patterns. Protistology 15:220–273

Kuris AM, Torchin ME, Lafferty KD (2002) *Fecampia erythrocephala* rediscovered: prevalence and distribution of parasitoid of the European shore crab, *Carcinus maenas*. J Mar Biol Assoc UK 82:955–960

Lafferty KD, Harvell CD, Conrad JM, Friedman CS and others (2015) Infectious diseases affect marine fisheries and aquaculture economics. Annu Rev Mar Sci 7: 471–496

Miller MA, Pfeiffer W, Schwartz T (2010) Creating the CIPRES Science Gateway for inference of large phylogenetic trees. In: Proc 2010 Gateway Computing Environments Workshop (GCE), p 1–8

Montagnani C, Le Roux F, Berthe F, Escoubas JM (2001) *Cg*-TIMP, an inducible tissue inhibitor of metalloproteinase from the Pacific oyster *Crassostrea gigas* with a potential role in wound healing and defense mechanisms. FEBS Lett 500:64–70

Morado JF (2011) Protistan diseases of commercially important crabs: a review. J Invertebr Pathol 106:27–53

Mullen TE, Russell S, Tucker MT, Maratea JL and others (2004) Paramoebiasis associated with mass mortality of American lobster *Homarus americanus* in Long Island Sound, USA. J Aquat Anim Health 16:29–38

Mullen TE, Nevis KR, O'Kelly CJ, Gast RJ, Frasca S (2005) Nuclear small-subunit ribosomal RNA gene-based characterization, molecular phylogeny and PCR detection of the *Neoparamoeba* from Western Long Island Sound lobster. J Shellfish Res 24:719–731

Newman MW, Ward GE (1973) An epizootic of blue crabs, *Callinectes sapidus*, caused by *Paramoeba perniciosa*. J Invertebr Pathol 22:329–334

Nishiguchi MK, Doukakis P, Egan M, Kizirian D and others (2002) DNA isolation procedures. In: DeSalle R, Giribet G, Wheeler W (eds) Techniques in molecular systematics and evolution. Birkhäuser, Basel, p 250–287

Nowak BF, Archibald JM (2018) Opportunistic but lethal: the mystery of paramoebae. Trends Parasitol 34: 404–419

Page FC (1970) Two new species of *Paramoeba* from Maine. J Protozool 17:421–427

Page FC (1987) The classification of 'naked' amoebae (Phylum Rhizopoda). Arch Protistenkd 133:199–217

Reynolds ES (1963) The use of lead citrate at high pH as an electron-opaque stain in electron microscopy. J Cell Biol 17:208–212

Ronquist F, Teslenko M, van der Mark P, Ayres DL and others (2012) MrBayes 3.2: efficient Bayesian phylogenetic inference and model choice across a large model space. Syst Biol 61:539–542

Saville DH, Irwin SWB (2005) A study of the mechanisms by which the cercariae of *Microphallus primas* (Jag, 1909) Stunkard, 1957, penetrate the shore crab *Carcinus maenas* (L). Parasitology 131:521–529

Sawyer TK (1976) Two new crustacean hosts for the parasitic amoeba, *Paramoeba perniciosa*. Trans Am Microsc Soc 95:271

Sawyer TK, MacLean SA (1978) Some protozoan diseases of decapod crustaceans. Mar Fish Rev 40:32–35

Sprague V, Beckett RL (1966) A disease of blue crabs (*Callinectes sapidus*) in Maryland and Virginia. J Invertebr Pathol 8:287–289

Sprague V, Beckett RL, Sawyer TK (1969) A new species of *Paramoeba* (Amoebida, Paramoebidae) parasitic in the crab *Callinectes sapidus.* J Invertebr Pathol 14:167–174

Stentiford GD (2008) Diseases of the European edible crab (*Cancer pagurus*): a review. ICES J Mar Sci 65: 1578–1592

Stentiford GD (2012) Diseases in aquatic crustaceans: problems and solutions for global food security. J Invertebr Pathol 110:139

Stentiford GD, Green M, Bateman K, Small HJ, Neil DM, Feist SW (2002) Infection by a *Hematodinium*-like parasitic dinoflagellate causes Pink Crab Disease (PCD) in the edible crab *Cancer pagurus.* J Invertebr Pathol 79: 179–191

Stentiford GD, Evans M, Bateman K, Feist SW (2003) Co-infection by a yeast-like organism in *Hematodinium*-infected European edible crabs *Cancer pagurus* and velvet swimming crabs *Necora puber* from the English Channel. Dis Aquat Org 54:195–202

Stentiford GD, Bateman KS, Longshaw M, Feist SW (2007) *Enterospora canceri* n. gen., n. sp., intranuclear within the hepatopancreatocytes of the European edible crab *Cancer pagurus.* Dis Aquat Org 75:61–72

Vogan CL, Costa-Ramos C, Rowley AF (2002) Shell disease syndrome in the edible crab, *Cancer pagurus* — isolation, characterization and pathogenicity of chitinolytic bacteria. Microbiology (Read) 148:743–754

Volkova E, Kudryavstev A (2021) A morphological and molecular reinvestigation of *Janickina pigmentifera* (Grassi, 1881) Chatton 1953 — an amoebozoan parasite of arrow-worms (Chaetognatha). Int J Syst Evol Microbiol 71, doi:10.1099/ijsem.0.005094

Volkova E, Kudryavtsev A (2017) Description of *Neoparamoeba longipodia* n. sp. and a new strain of *Neoparamoeba aestuarina* (Page, 1970) (Amoebozoa, Dactylopodida) from deep-sea habitats. Eur J Protistol 61: 107–121

Volkova E, Völcker E, Clauß S, Bondarenko N, Kudryavtsev A (2019) *Paramoeba aparasomata* n. sp., a symbiont-free species, and its relative *Paramoeba karteshi* n. sp. (Amoebozoa, Dactylopodida). Eur J Protistol 71: 125630

Young ND, Crosbie PB, Adams MB, Nowak BF, Morrison RN (2007) *Neoparamoeba perurans* n. sp., an agent of amoebic gill disease of Atlantic salmon (*Salmo salar*). Int J Parasitol 37:1469–1481

Young ND, Dyková I, Crosbie PB, Wolf M, Morrison RN, Bridle AR, Nowak BF (2014) Support for the coevolution of *Neoparamoeba* and their endosymbionts, *Perkinsela amoebae*-like organisms. Eur J Protistol 50:509–523

Editorial responsibility: Jeffrey Shields, Gloucester Point, Virginia, USA
Reviewed by: B. Nowak and 2 anonymous referees

Submitted: July 27, 2021
Accepted: April 7, 2022
Proofs received from author(s): June 22, 2022